[EA]Transgressive Reworking and its Impact on Sandstone Porosity Improvement: The Vivian Formation, Marañón Basin, Northern Peru*

Oscar R. López-Gamundi[1] and Cecilia López-Gamundi[2]

Search and Discovery Article #11211 (2019)**
Posted May 6, 2019

*Adapted from extended abstract based on poster presentation given at 2018 AAPG Annual Convention & Exhibition, Salt Lake City, Utah, May 20-23, 2018

[1]P1 Consultants, Houston, Texas (olopez-gamundi@p1consultants.com)
[2]ConocoPhillips School of Geology and Geophysics, University of Oklahoma, Norman, Oklahoma

Abstract

The craton-derived, quartz-rich sandstones of the Upper Cretaceous Vivian Formation are the most important reservoirs in the prolific Marañón foreland basin of northern Perú. Porosity versus depth analysis for the dominantly fluvial Vivian sandstones shows a simple trend of decreasing porosity with depth, which suggests that overburden stress is the dominant factor that determines porosity reduction in the basin. However, anomalously high porosities at significant depths which substantially deviate from the depth versus porosity regional trend were identified in few wells. Gamma Ray (GR)-based log signatures indicate that those intervals with anomalously high porosities are identified in thin, fining upward (dirtying upward) successions resting on slightly coarsening up (cleaning up), blocky or funnel-shaped GR electrofacies. The surface which marks the change from the fluvial/shallowing-upward strata below to the deepening-upward, transgressive strata above is considered a maximum regressive surface (MRS). The interval bound between the MRS (coplanar with the initial flooding or transgressive surface, ITS) and the maximum flooding surface (MFS) defines the transgressive systems tract (TST).

TST thickness variation along a depositional dip direction can be interpreted as an estimate of transgressive reworking. This process is effective when rates of net deposition and relative sea level change are in equilibrium, allowing extensive reworking of underlying sands. SE-NW oriented depositional dip cross sections across the Vivian Formation illustrate the transition from a proximal, sand-rich TST to a more distal, sand poor TST. Depending on the location along depositional dip, the MFS may be located very close to or almost coincident with the ITS (= MRS) in the more proximal locations or be significantly decoupled basinward, leading to a shale richer TST. Porosity values in the early TST sandstones may be significantly higher (up to 8-10%) than the fluvial blocky sands, suggesting transgressive reworking of the underlying sand-rich deposits. This porosity increase detected in the thin, transgressive sandstones of the Vivian Formation indicates that the decoupling of the ITS and MFS can be used as an estimate of wave reworking during transgressions.

The Vivian Sandstones in the Marañón Basin

The craton-derived, quartz-rich sandstones of the Upper Cretaceous Vivian Formation constitute the most important reservoirs in the Marañón Basin of northern Perú (Figure 1; Del Solar, 1982; Augusto et al., 1990; Lay, 1991; Alvarez Calderón, 1997; Lay and Becerra, 1997; Zamora and Willy, 2018).

The Vivian Formation (Figure 2, Figure 3 and Figure 4) shows a regional thickening, from 50-100 m (~160-330 ft) in the north/northeast to over 200 m (~650 ft) in the south/southwest (Figure 3). Although many wells have penetrated the Vivian reservoirs in the Marañón Basin, fewer have penetrated in the Santiago and Huallaga basins (Figure 5). This formation consists of two genetic sequences. The depositional setting transitions from a sandy, low-sinuosity, fluvial to a shoreface and open shelf marine environment along a NE to W and NW transect (Figure 3).

In the proximal, east Marañón, the Vivian Formation consists entirely of aggradational terrestrial fluvial deposits mostly composed of massive moderately sorted, fluvial sandstones that range in thickness from 12 to 60 m (~ 40-200 ft). The Vivian Formation is further subdivided in central and west Marañón into two sand-rich units (Lower Vivian or Vivian A, and Upper Vivian or Vivian B) with an intervening thin, mudprone interval (Figure 4). The lower Vivian Formation (Vivian A) consists mostly of cross-bedded, fine- to medium-grained sandstones, interpreted as stacked or amalgamated fluvial channels (Kummel, 1948; Macellari, 1988; Augusto et al., 1990; Alvarez-Calderon, 1999; Marky and Grosso, 2010; Ramdoski and Hearn, 2010).

Vertical and lateral lithofacies variations across the Marañón Basin are reflected in the GR log-based electrofacies domains identified in the Vivian Formation (Figure 6 and Figure 7). The tripartite subdivision of the unit (Vivian A, shale-prone interval, and Vivian B) is clear in the intermediate and distal electrofacies, whereas the intervening shale-prone interval sands out toward the proximal portion of the basin merging both sand prone intervals A and B (Figure 6). The proximal domain is made up of blocky, GR log-based electrofacies.

The Vivian Formation is overlain by the transgressive, mud-prone Cachiyacu Formation which acts as a regional seal in the central and distal portions of the basin. Cross sections along the depositional strike (Figure 8) and dip (Figure 9) clearly show three main electrofacies domains (Figure 6). On the distal domain (distal electrofacies), a clear fining upward trend in the GR suggests a marine transgression with an accompanying deepening of the basin at the Vivian B-Cachiyacu transition.

Transgressive Reworking

Anomalously high porosities at significant depths which deviate substantially from the depth versus porosity regional trend have been identified by Lopez-Gamundi and Lopez-Gamundi (2018) (Figure 10). In northern Marañón, the Vivian sandstones at the Situche Central-2X well (Figure 5) show two distinct porosity values. The fluvial, blocky GR electrofacies Vivian A sandstone has a porosity value that fits the regional trend (Figure 11). The overlying Upper Vivian sandstone (High Permeability (HP) streak, has an anomalously high porosity value compared to that of the underlying background fluvial, Vivian A sandstone (Figure 11).

The overlying Upper Vivian sandstone (High Permeability (HP) streak, Figure 11) has an anomalously high porosity value compared to that of the underlying background fluvial, Vivian A sandstone (Figure 10 and Figure 11). A similar porosity shift is identified for the Vivian sandstones in the adjacent Santiago Basin in the Tanguitza 1X well. A distinct, thin 3 m (10 ft) Vivian sandstone, designated the "Bubble Sand" (equivalent to the Vivian B), separated from the principal Vivian sandstone ("Blocky sand" or Vivian A) by an approximately 30 m (100 ft) - thick shale interval, was found toward the top of the Formation in the Tanguitza 1X well (Figure 11). The "Bubble Sand" has large, interconnected pore space, is fine-grained and moderately well sorted and exhibits the best porosities (up to 17%). Conversely, the main blocky sandstone ("Blocky sand") is coarse-grained and poorly sorted with reduced intergranular porosity due to compaction and, to a lesser degree, cementation.

The maximum regressive surface (MRS), coplanar with the initial transgressive surfaces (ITS), has been placed at the decreasing to increasing GR trend transition (cf. Figure 12). This change in the GR trend is interpreted to reflect a transition to deepening-upward environments. Wave reworking is present in the early transgressive systems tract (ETST) interval, while the LTST is dominated by sedimentation below wave base capped by the maximum flooding surface.

Conclusions

1) Anomalously high porosities at significant depths showing a substantial diversion from the Vivian depth versus porosity regional trend were identified in a few wells (i.e. Situche central 2X and Tanguitza 1X).

2) GR-based log signatures indicate that those intervals with anomalously high porosities are found within thin, fining upward (dirtying upward) successions resting on slightly coarsening upward (cleaning upward), blocky or funnel-shaped GR electrofacies. Porosity values in the early TST sandstones may be significantly higher (up to 8-10%) than the fluvial blocky sands, suggesting transgressive reworking of the underlying sand-rich deposits.

3) This porosity increase detected in these thin, transgressive sandstones of the Vivian Formation (Vivian B interval) indicates that the decoupling of the ITS and MFS can be used as an estimate of wave reworking during transgressions.

References Cited

Alvarez Calderón, E., 1997, The Cretaceous Chonta-Vivian Petroleum System Block 1AB, Sub Andean Marañón Basin, Perú: VI Simposio Bolivariano, Bogotá, Tomo 1, p. 351-370.

Augusto, M., C. Ardiles, and C. Orosco, 1990, Geología del yacimiento Shiviyacu: Boletín Sociedad Geológica del Perú, v. 81, p. 63-80.

Del Solar, C., 1982, Ocurrencia de hidrocarburos en la Formación Vivian, nordoriente peruano: I Simposio Bolivariano, Bogotá, Tomo 1, 8, 33 p.

Embry, 2008, Practical Sequence Stratigraphy VI, The Material-based Surfaces of Sequence Stratigraphy, Part 3: Maximum Flooding Surface and Slope Onlap Surface: Reservoir, v. 10, p. 36-41.

Kummel, B., 1948, Stratigraphic studies in Peru, American Journal of Science, v. 248, p. 249-263.

Lay, V., 1991, Ocurrencias de petróleo en el Cretáceo de la Cuenca de Marañón: VII Congreso Peruano de Geología, Sociedad Geológica del Perú, Volumen de Resúmenes Extendidos, Tomo I, p. 307-311.

Lay, V., and A. Becerra, 1997, Exploration and development of oil fields in the Northern Marañón Basin-Perú: VI Simposio Bolivariano, Bogotá, Tomo 1, p. 371-393.

Lopez-Gamundi, O., and C. Lopez-Gamundi, 2018, Exhumation of a proximal foredeep and associated wedge-top basin evidenced by porosity versus depth trends: The Upper Cretaceous Vivian Sandstones in northwestern Marañón and Santiago Basins (Peru), *in* G. Zamora, K.R. McClay, and V.A. Ramos, eds., Petroleum basins and hydrocarbon potential of the Andes of Peru and Bolivia: AAPG Memoir 117, p. 251-270.

Macellari, C.E., 1988, Cretaceous paleogeography and depositional cycles of western South America, Journal of South American Earth Sciences, v. 1, p. 373-418.

Marsky, T., and S. Grosso, 2010, Caracterización sedimentológica y petrofísica de la Formación Vivian en el Campo Cashiriari, área Camisea, Cuenca Ucayali, Peru in XV Congreso Geológico Peruano, Simposio Exploración en el Subandino 27, October 1, Cusco, Peru, 4 p.

Mathalone, J.M.P., and R.M. Montoya, 1995, Petroleum geology of the sub-Andean basins of Perú, *in* A.J. Tankard, R. Suárez Soruco, and H.J. Welsink, eds., Petroleum basins of South America: AAPG Memoir 62, p. 423-444.

Radomski, M.A., and M. Hearn, 2010, Sedimentology of the Lower Vivian Formation: A widespread lowstand fluvial system? Marañón Basin, Perú: Canadian Society of Exploration Geophysicists, Conference Core Abstracts, 1 p.

Zamora, G., and G. Willy, 2018, The Marañón Basin: Tectonic evolution and paleogeography, *in* G. Zamora, K.R. McClay, and V.A. Ramos, eds., Petroleum basins and hydrocarbon potential of the Andes of Peru and Bolivia: AAPG Memoir 117, p. 121-144.

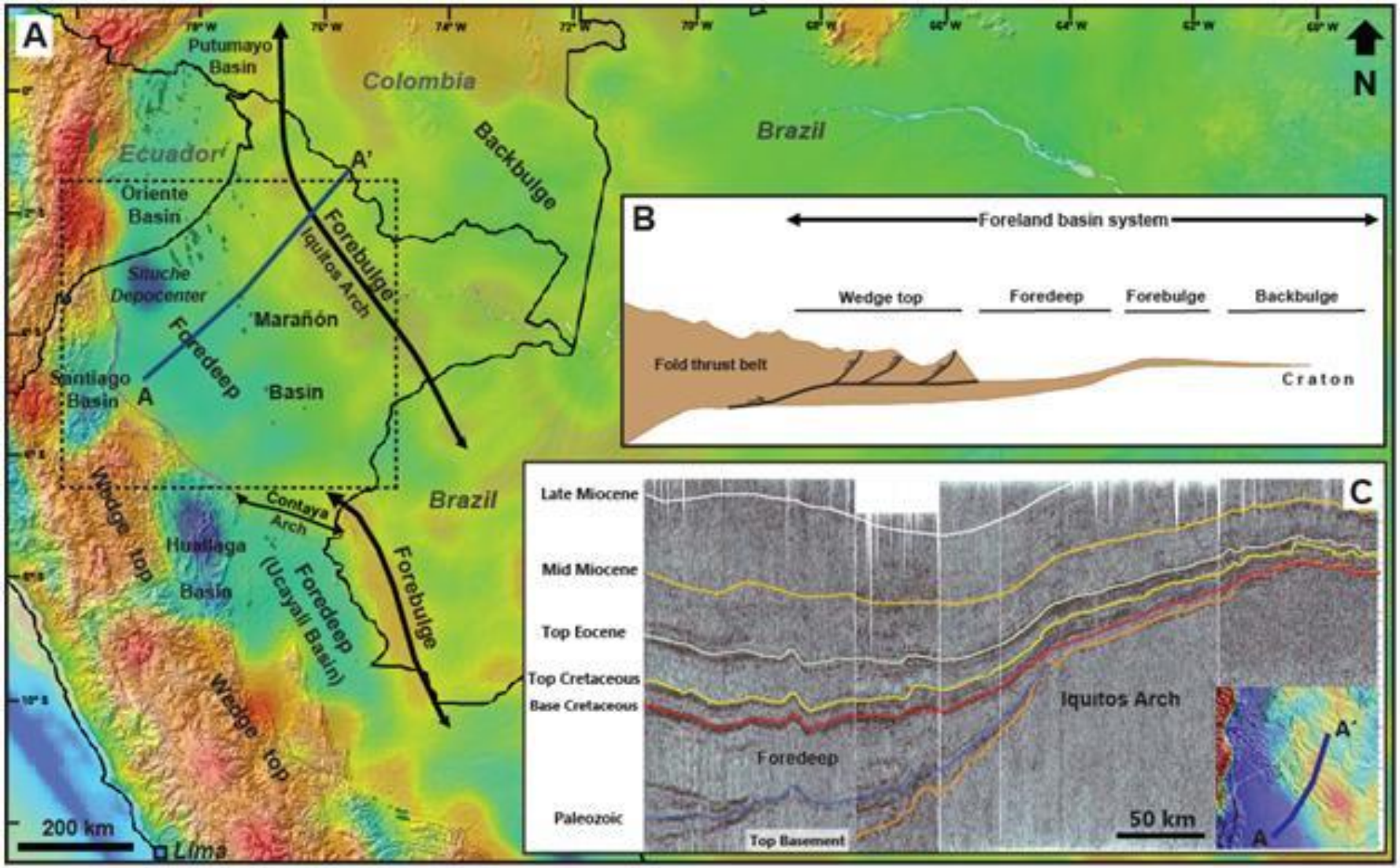

Figure 1. (A) Gravity map with the Marañón-Oriente-Putumayo province across Peru, Ecuador, and Colombia with associated wedgetop Santiago and Huallaga basins west of the Marañón and Ucayali basins respectively. Stippled rectangle indicates area of study. (B) Tripartite subdivision of a foreland basin system (backbulge, forebulge and foredeep) developed during the Tertiary. (C) Dip seismic section (A-A') in northern Marañón Basin comprising the foredeep and forebulge high (Iquitos Arch).

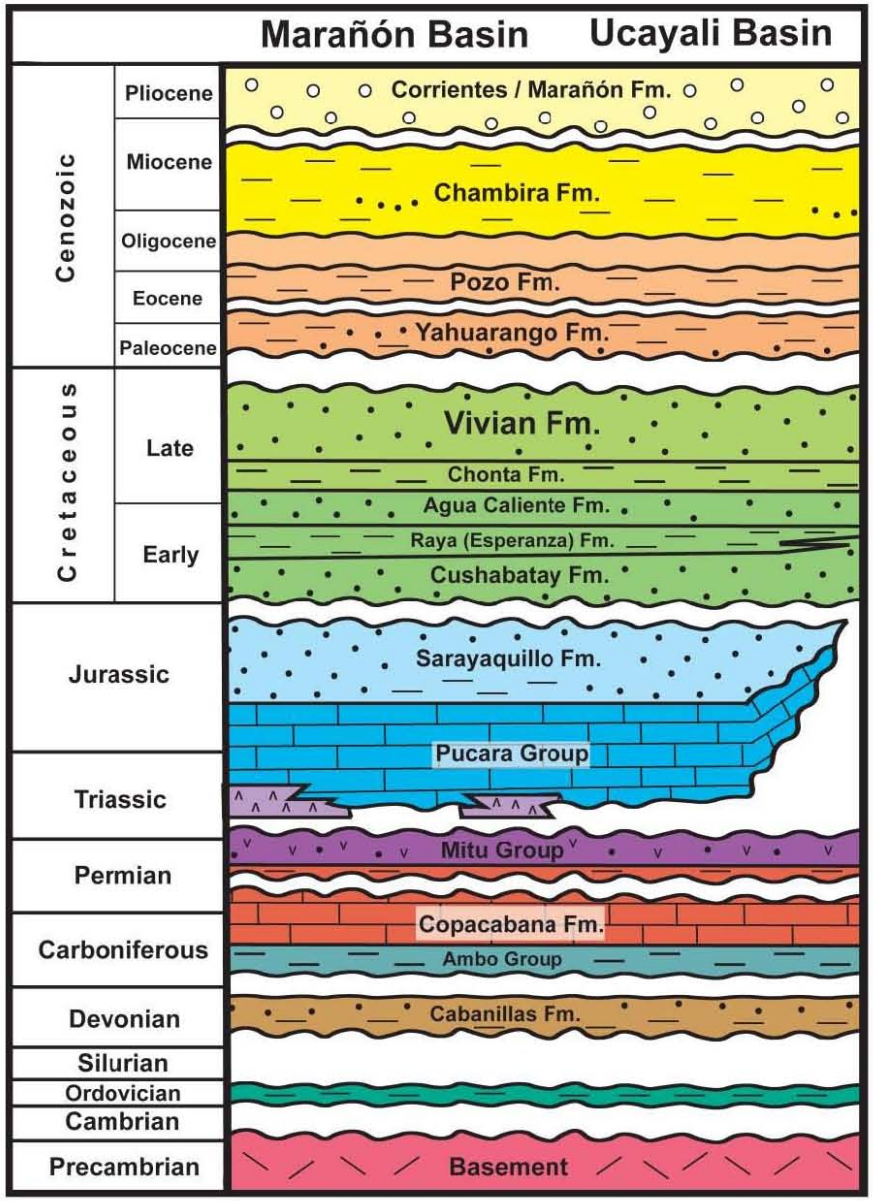

Figure 2. Stratigraphy of the Sub-Andean Marañón and Ucayali basins of Peru (from Mathalone and Montoya, 1995). The sandstones of the Cretaceous Vivian, Agua Caliente, and Cushabatay formations are the main reservoirs. The north Marañón Sub-Basin is differentiated from the south Marañón Sub-Basin by their source rocks (principally the Chonta Group for the north sub-basin and the Pucará Group for the south Sub-Basin). The Vivian Formation transitions into the Cachiyacu Formation shales towards the center of the basin and is unconformably overlain by the Yuarango Formation along the western basin margin.

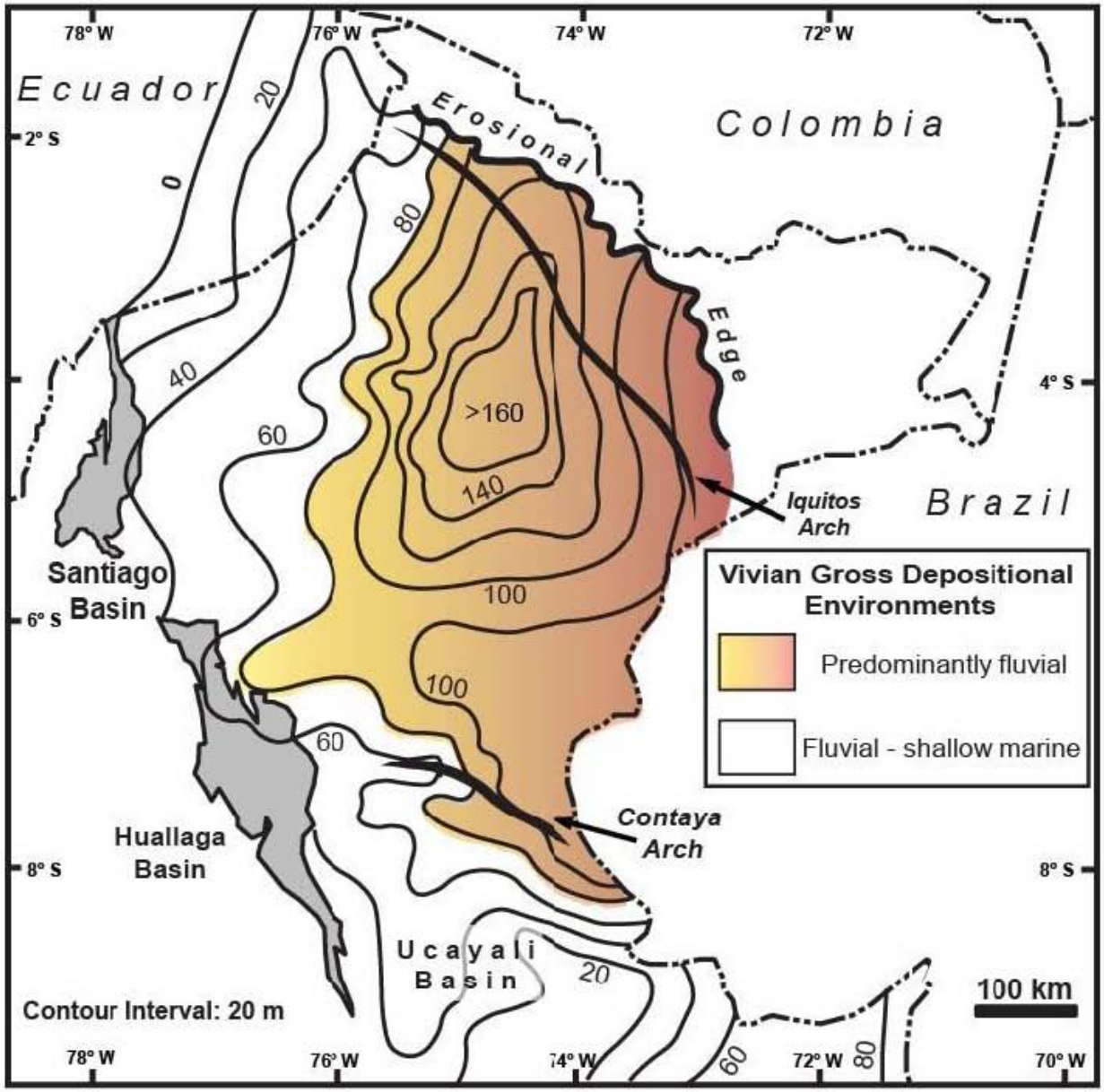

Figure 3. Regional isopach map of the Vivian Formation showing thinning toward the Oriente Basin (Ecuador) and NW Marañón Basin (modified from Mathalone and Montoya, 1995). The Upper Vivian is overlain by transgressive marine shales (Cachiyacu Formation) toward the northwest and west. Marine influence increases distally toward those directions, particularly for the Upper Vivian, which is evidenced by distinctive changes in electrofacies. The Vivian Formation is also present in the Santiago and Huallaga basins where it has been upthrusted by the Andean Orogeny.

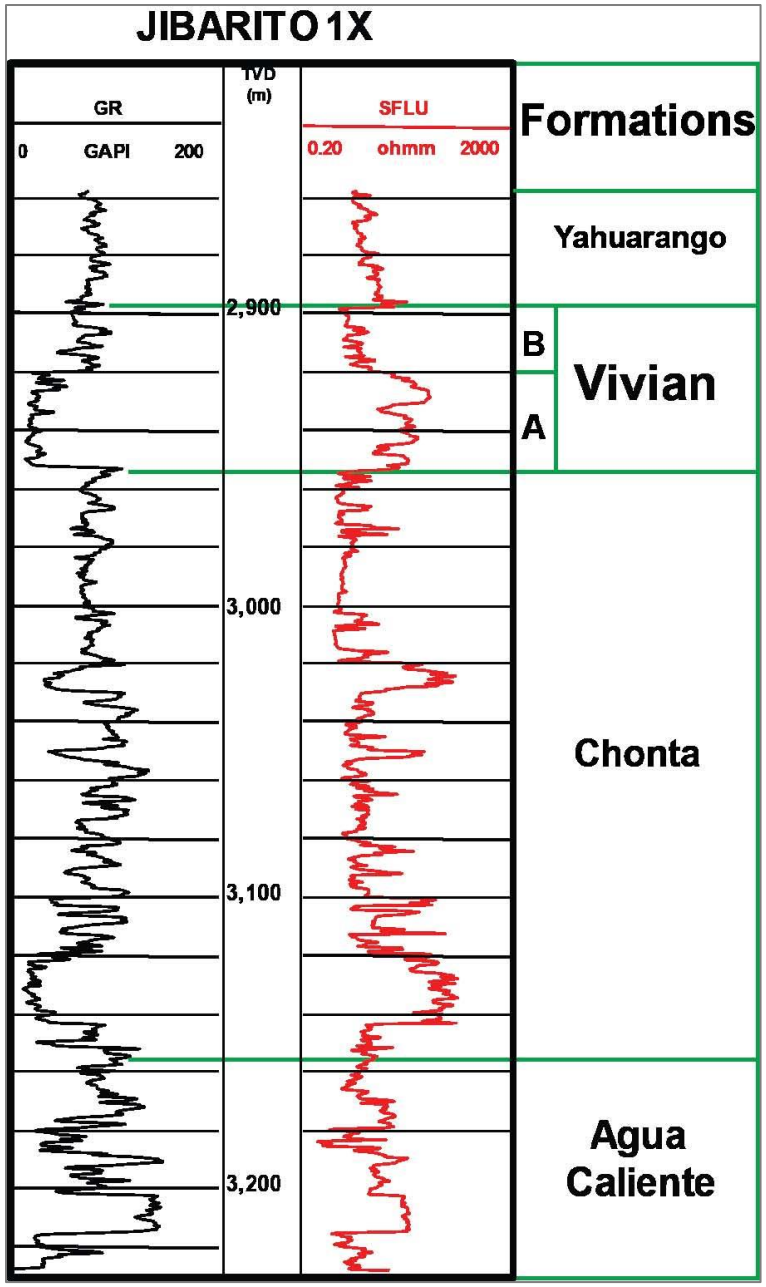

Figure 4. Cretaceous section in the Jibarito 1X well. The Vivian Formation is subdivided into (1) the Lower Vivian (or Vivian A), which is characterized by fluvial sandstones, followed by (2) a shale-prone interval which grades upward into (3) the Upper Vivian finer-grained sandstones (Vivian B with shallow marine influence towards the west and northwest).

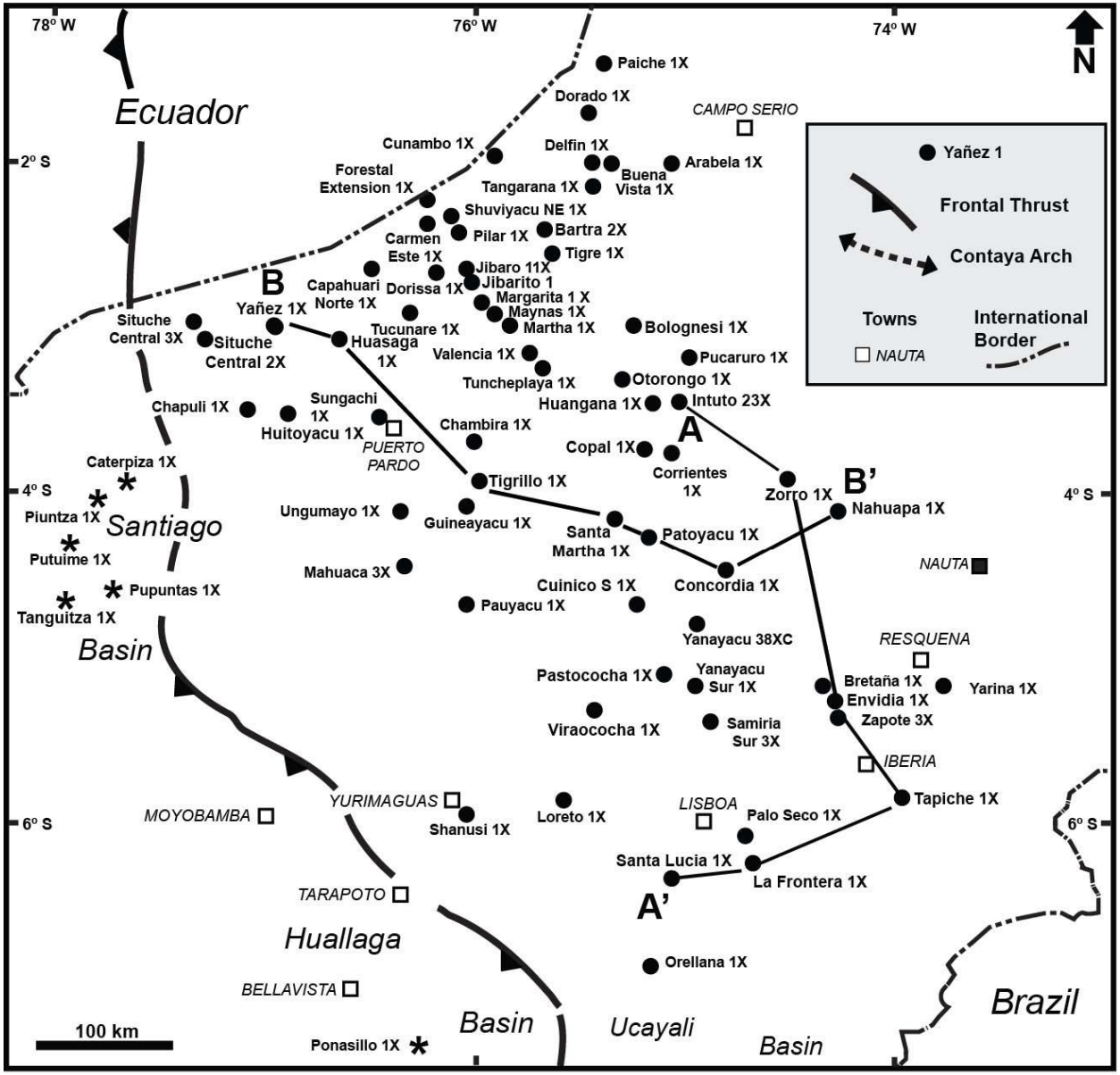

Figure 5. Location map of Marañón Basin wells used in this study and by Lopez-Gamundi and Lopez-Gamundi (2018) to calculate porosity versus depth regional trend (represented in black dots); see Figure 10. The wells which encountered a complete Vivian Formation section in the Santiago Basin are Caterpiza 1X, Piuntza 1X, Putuime 1X, Pupuntas 1X and Tanguitza 1X (well locations are represented by asterisks). Location of cross sections A-A' (Figure 8) and B-B' (Figure 9) shown.

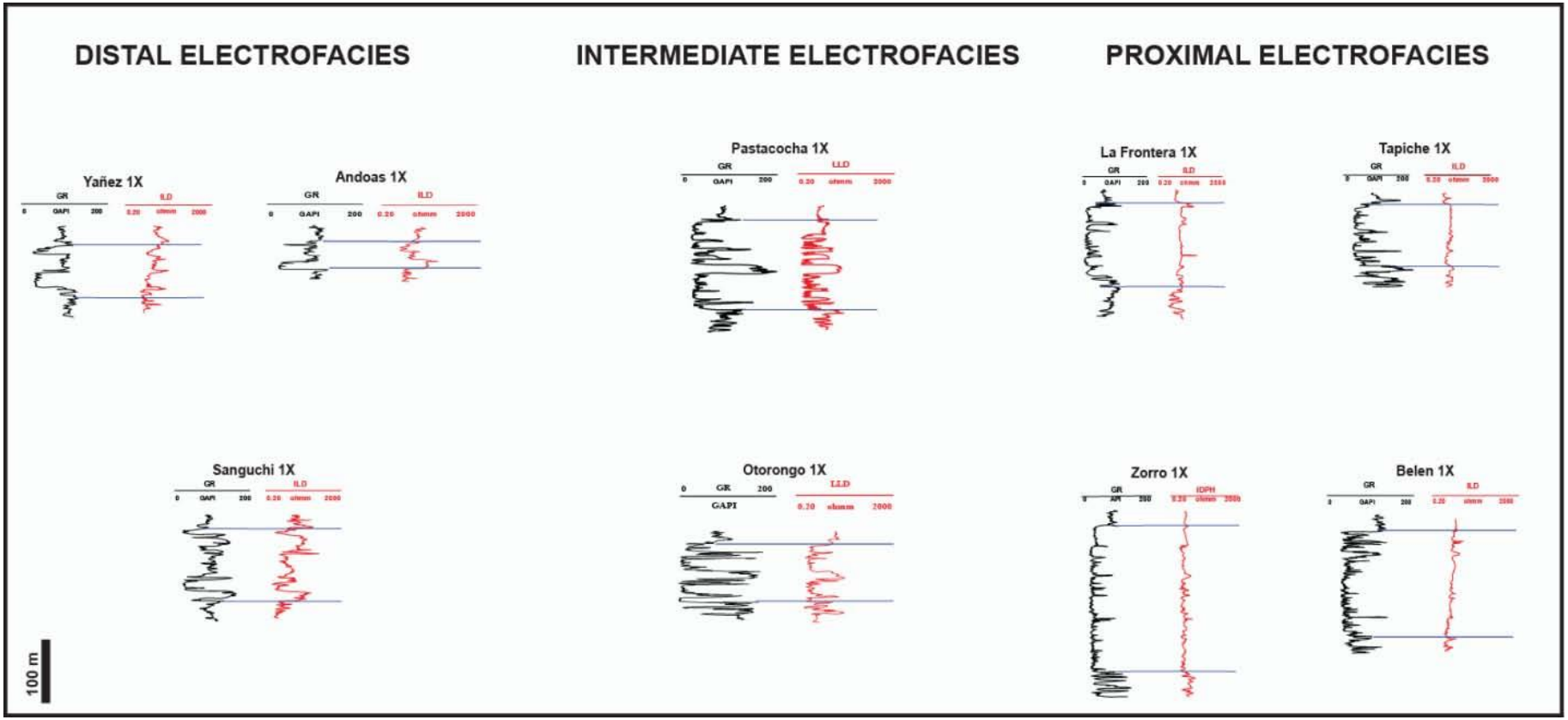

Figure 6. GR log-based electrofacies domains in the Vivian Formation across the Marañón Basin. The tripartite subdivision of the three units (Vivian A, shale prone interval, and Vivian B) is clear in the intermediate and distal electrofacies, whereas the intervening shale-prone interval sands out toward proximally, merging both sand-prone A and B intervals. Location of wells in Figure 5.

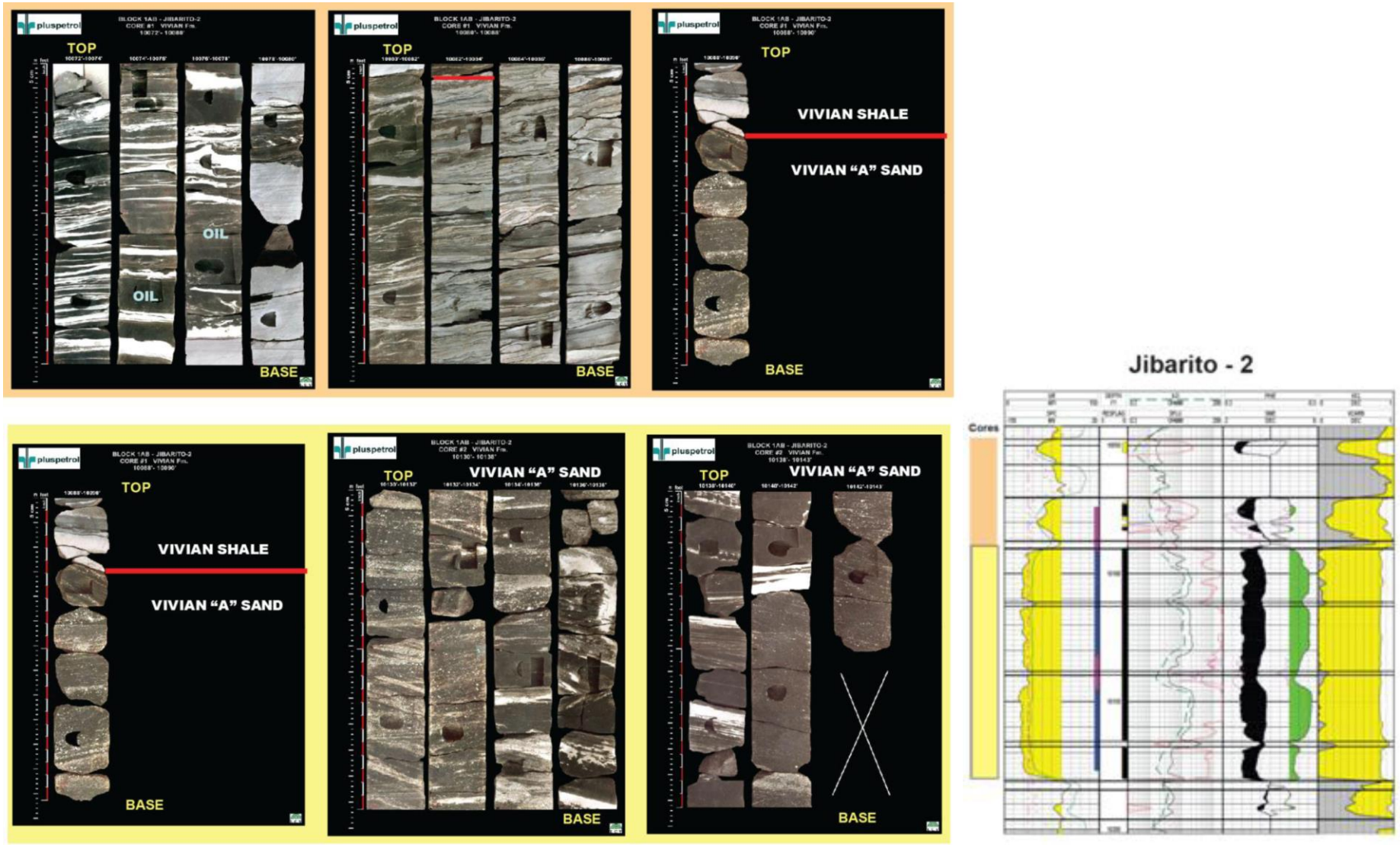

Figure 7. Cores from the Vivian A and B intervals at Jibarito-2 well in Jibarito Field, north Marañón Basin. The Vivian A section is dominated by coarse- to medium-grained sandstones with a blocky GR-based log signature; the Vivian B section is characterized by a heterolithic, thin-bedded association of fine-grained sandstones and mudstones. Oil-stained sandstones appear dark grey in the coarser- grained intervals and light grey in the finer grained intervals. Courtesy of Pluspetrol.

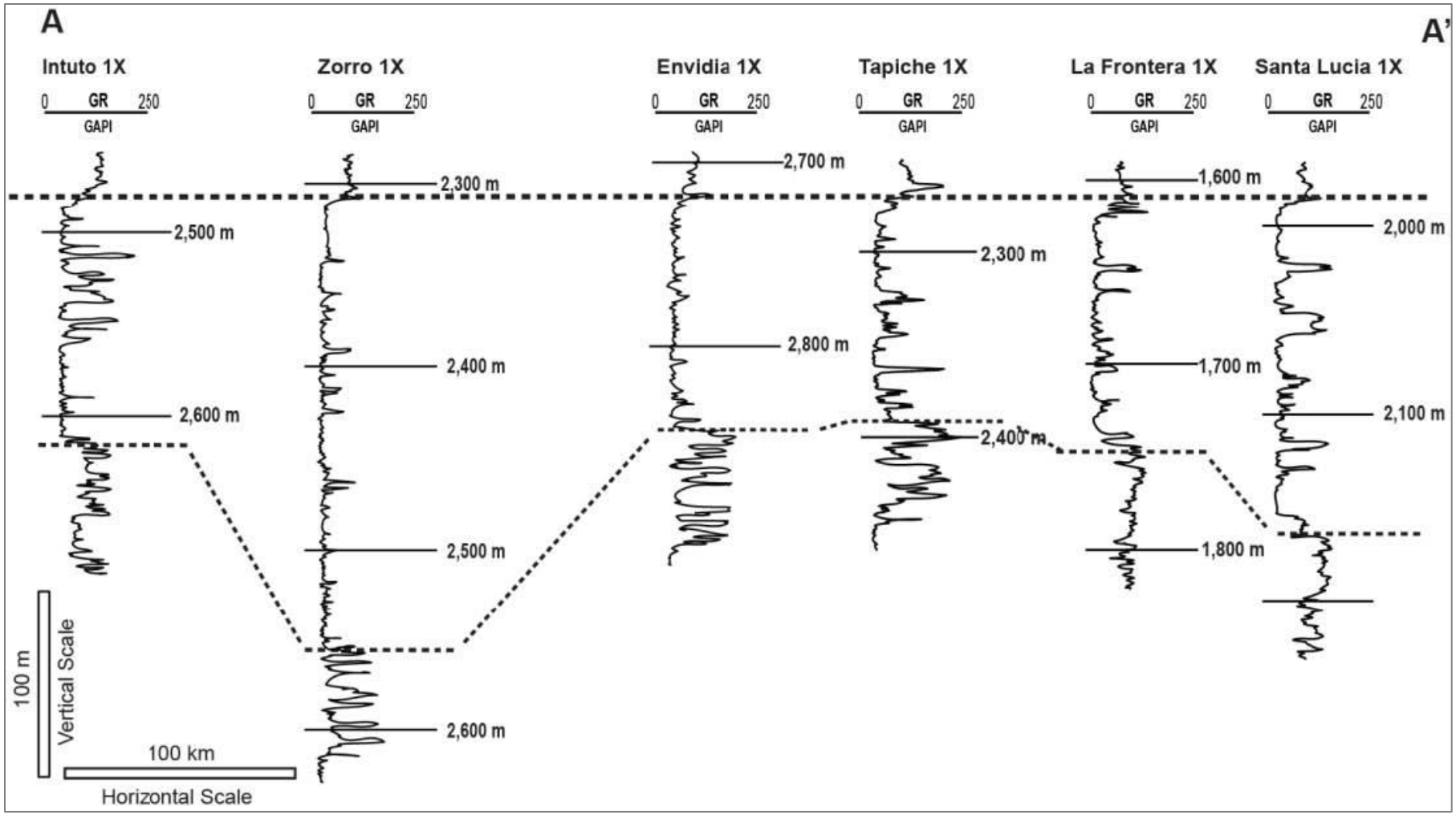

Figure 8. Proximal strike cross section of Vivian Formation. Note blocky GR-based log signature of electrofacies. Location of cross section in Figure 5.

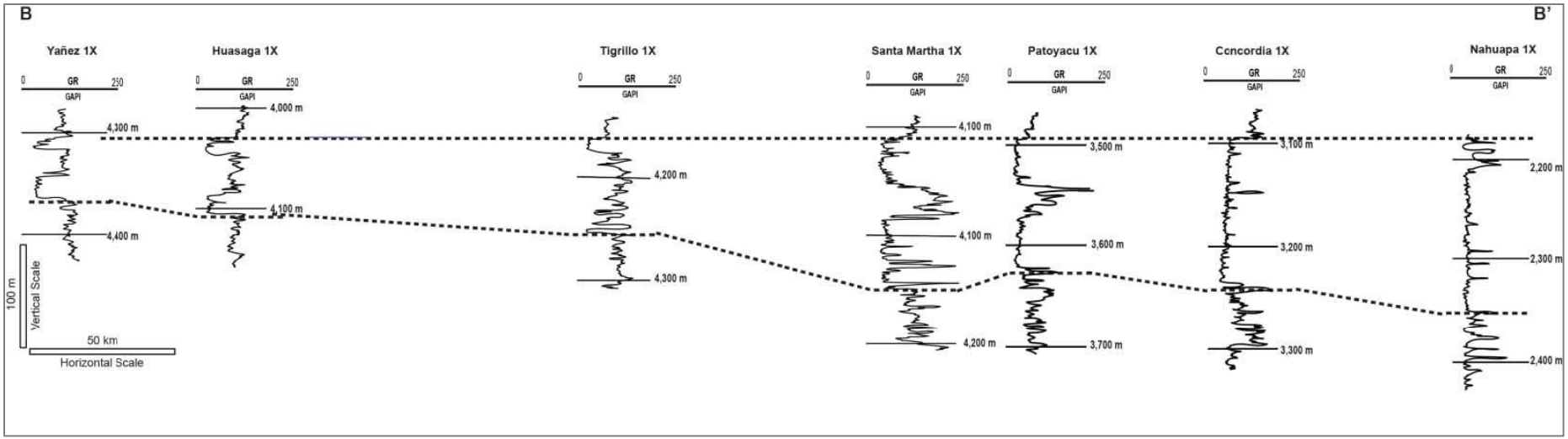

Figure 9. Dip oriented cross section of Vivian Formation flattened on the base of the Cachiyacu Formation. Note both (1) the blocky GR log signature of the entire Vivian Formation towards the basin margin (i.e. Nahuapa 1X, Concordia 1X) and the lateral transition to the blocky Vivian A (2) the shale-prone interval and serrate fining upward log signature of Vivian B distally (i.e. Yañez 1X). Location of cross section in Figure 5.

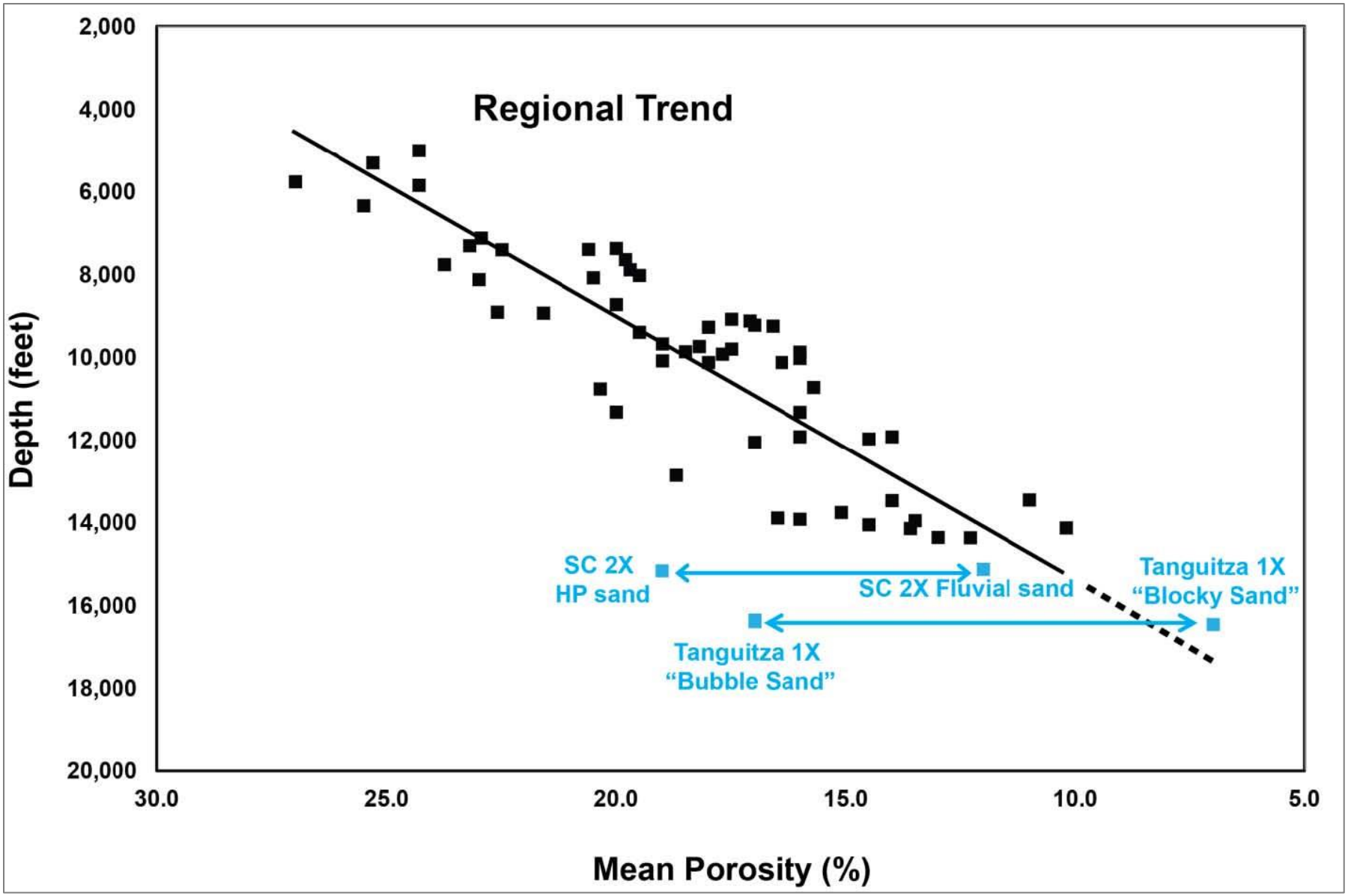

Figure 10. Porosity versus depth diagram showing regional trend for the Vivian sandstones, Marañón Basin (from Lopez-Gamundi and Lopez-Gamundi, 2018). Note diversion from regional trend of HP sand in Situche Central 2X well (northwest Marañón) and Bubble sand in Tanguitza 1 X well (Santiago Basin). See Figure 5 for location of wells.

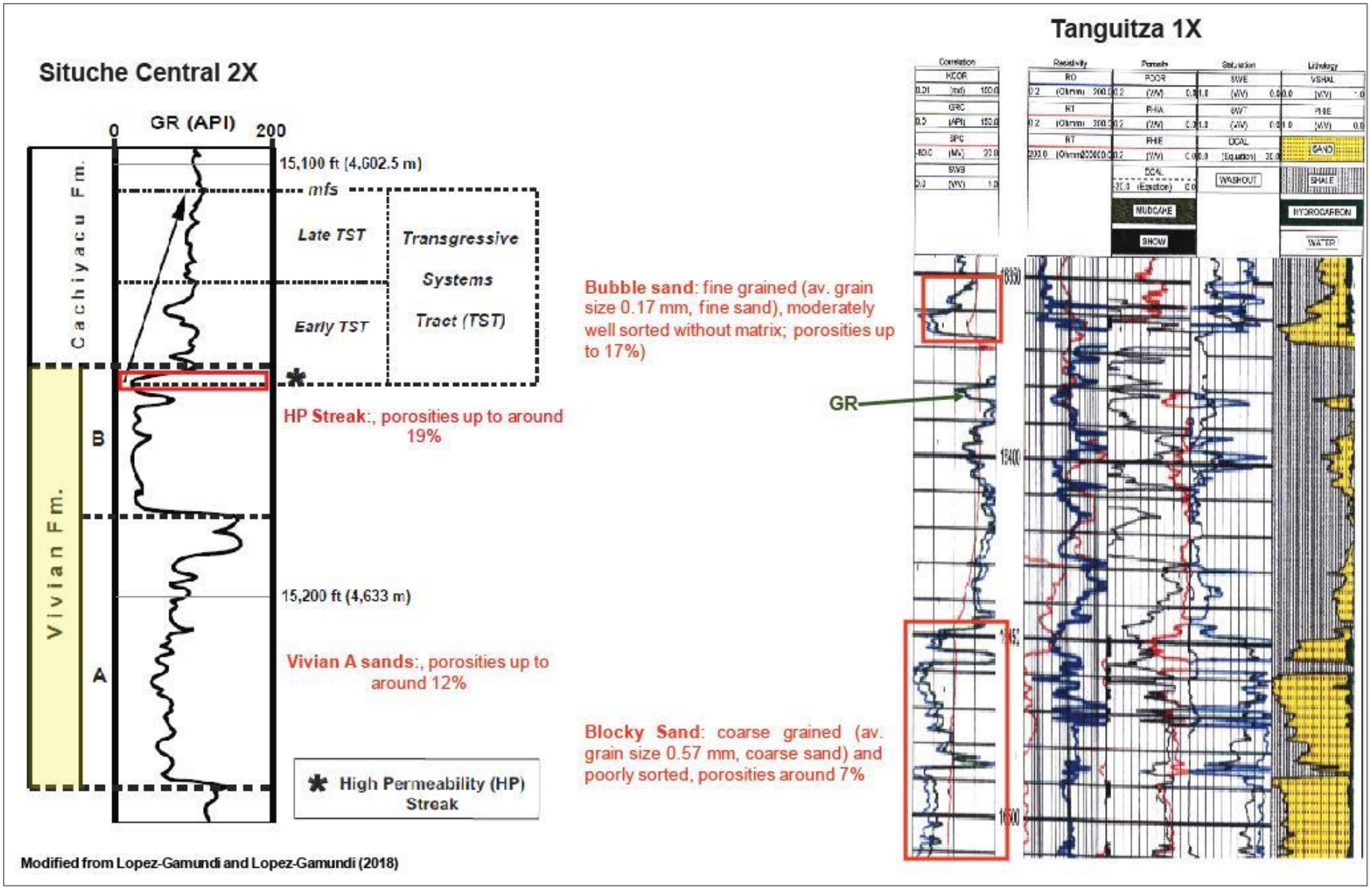

Figure 11. Examples of reworked Vivian sandstones in Situche Central 2X and Tanguitza 1X well.

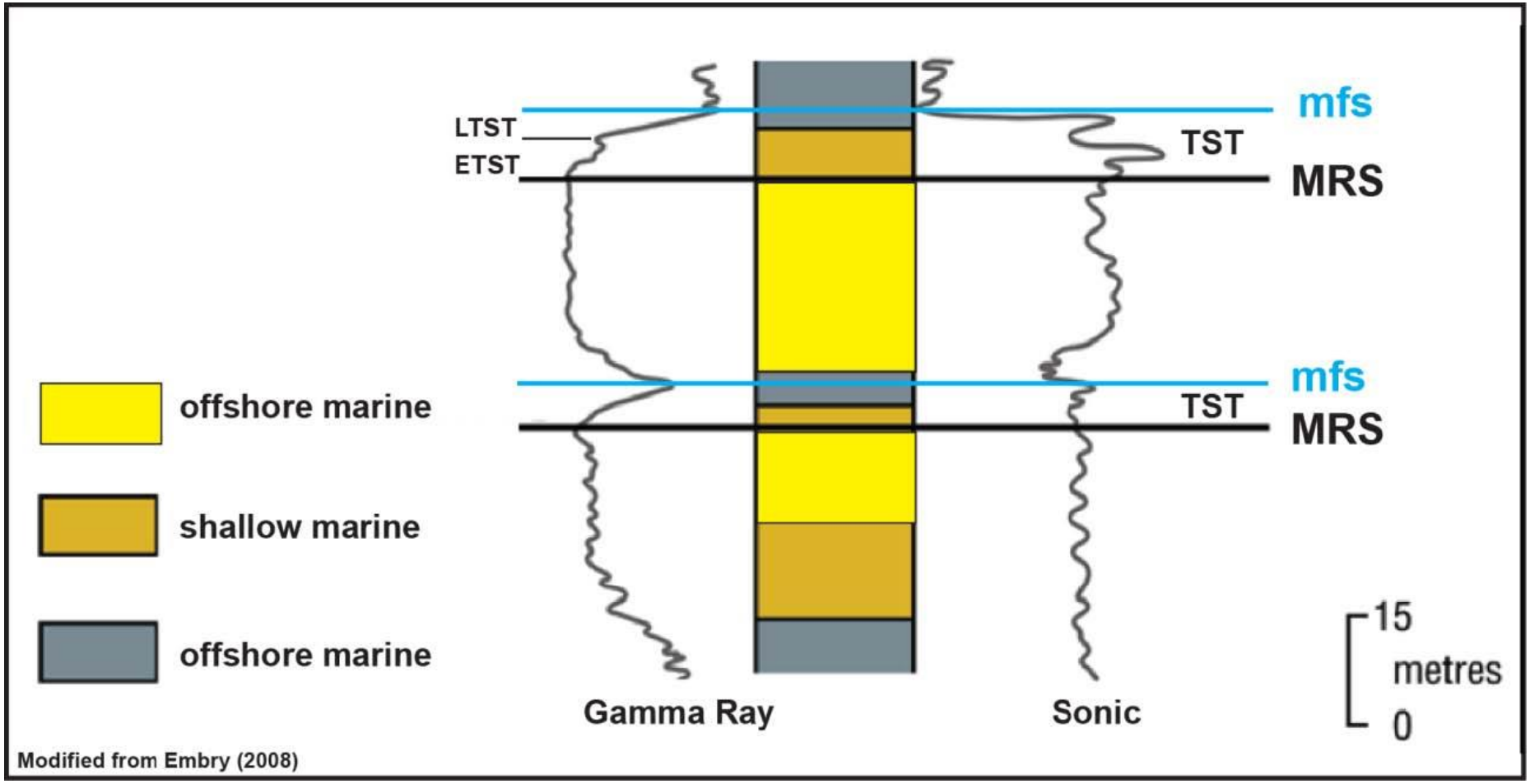

Figure 12. Definition of early (ETST) and late (LTST) transgressive systems tract (Embry, 2008). Two maximum regressive surfaces (MRS), coplanar with the initial transgressive surfaces (IRS), have been placed at the Gamma Ray (GR) log trend transition from decreasing GR to increasing GR. This change in the GR trend is interpreted to reflect a change from shallowing-upward (decreasing clay content) to deepening-upward (increasing clay content). Wave reworking is present in ETST interval, while the LTST is dominated by sedimentation below wave base capped by the maximum flooding surface (mfs). Compare with similar Vivian examples in Figure 11.